JOURNAL OF SPACECRAFT AND ROCKETS
Vol. 43, No. 6, November–December 2006

Collision Risk Posed to the Global Positioning System by Disposed Upper Stages

A. B. Jenkin* and R. A. Gick†
The Aerospace Corporation, Los Angeles, California 90009-2957

DOI: 10.2514/1.15398

Block IIF satellites in the Global Positioning System will be directly inserted into the constellation by the Evolved Expendable Launch Vehicle. However, the upper stages will not be able to relocate to recommended disposal orbits above the constellation and will remain at least partially in the constellation. The purpose of this study is to determine the collision risk posed to the operational constellation by the disposed upper stages. The analysis includes the effect of the long-term eccentricity growth of the upper-stage disposal orbits. Because eccentricity growth is very sensitive to the initial conditions of the disposal orbit, it is necessary to account for the statistical spread in the initial conditions. This spread is caused by dispersions in launch vehicle and upper-stage maneuvers and by inability to predict the sequence of orbit planes in which disposal will occur. A Monte Carlo procedure was used to quantify this statistical variation. Only one version of the launch vehicle was considered here. Study results include 5-, 50-, and 95-percentile profiles over 200 years of cumulative collision probability and cumulative number of collision avoidance maneuvers that may have to be performed by operational constellation satellites.

Nomenclature

A_{cc} = average collision cross-sectional area between the upper stage and constellation satellites, m^2 (convert to km^2 for unit consistency in equations)
h_{us} = altitude of the upper stage, km
$N_C(t)$ = average number of collisions at time t
$p_C(t)$ = cumulative collision probability at time t
R_{cc} = collision radius, m (convert to km for unit consistency in equations)
R_m = miss distance threshold for triggering an avoidance maneuver, m
r_{us} = position vector of the upper stage, km
T_p = orbital period, s
t = current time point, s
t_L = long scale time, years (convert to s for unit consistency in equations)
t_0 = disposal epoch, s
v = relative velocity between the upper stage and constellation satellite averaged over all constellation members and time, km/s
$x = [a, e, i, \Omega, \omega]$ = vector of five slowly varying classical orbital elements
$\rho(h)$ = constellation spatial density distribution over altitude, number/km^3
$\rho(r_{us})$ = constellation spatial density at the position of the disposed upper stage, number/km^3
τ = dummy time variable for integration, s
τ_S = short time scale dummy variable for integration, s
τ_L = long time scale dummy variable for integration, years (convert to s for unit consistency in equations)

Presented as Paper IAC-03-IAA.5.3.01 at the International Astronautical Congress 2003, Bremen, Germany, 29 September–3 October 2003; received 4 January 2005; revision received 2 November 2005; accepted for publication 2 November 2005.

*Senior Engineering Specialist, Astrodynamics Department; Alan.B.Jenkin@aero.org,.Associate Fellow AIAA.

†Senior Member of the Technical Staff, Astrodynamics Department; currently Senior Engineering Specialist with Performance Modeling and Analysis Department, Chantilly Office; RAnne.Gick@aero.org. Member AIAA.

I. Introduction

DEBRIS mitigation guidelines, policy directives, and instructions now exist within the U.S. government that address end-of-life disposal of satellites and upper stages. As an example, the U.S. Government Debris Mitigation Standard Practice recommends that all vehicles operating in medium Earth orbit (MEO) be moved to altitude regions at least 500 km above or below semisynchronous orbit. (Throughout this paper altitudes will be given in terms of height above the ideal, 12-hour semisynchronous circular orbit with radial distance from the center of the Earth of 26,559.7 km). These disposal regions were selected with the intent to preclude the possibility of collision between the disposed vehicle and operational members of the Global Positioning System (GPS) constellation.

Historically, compliance with this guideline by GPS has not been difficult. GPS satellites have had adequate remaining propellant at end of life to raise perigee to altitudes between 750 and 1350 km. The upper stages have remained on highly eccentric transfer orbits with perigees low enough for atmospheric drag to restrict orbital lifetime. The satellites have used an integrated apogee kick motor to raise perigee and circularize the orbit.

Starting with Block IIF, the satellites will be directly inserted into the operational constellation by the Evolved Expendable Launch Vehicle (EELV). However, due to design restrictions, the upper stage will not be able to move itself to the recommended disposal regions. At best, the upper stage can achieve restricted modifications to the disposal orbit's elements via a sequence of post-separation maneuvers. It will not be possible to fully remove the upper stages from the altitude band of the operational constellation.

The end-of-life disposal of satellites and upper stages has been a focus of study at The Aerospace Corporation. Studies of GPS satellite and upper-stage disposal have been performed for the GPS Program, the EELV Program, and the Center for Orbital and Reentry Debris Studies [1–5]. Chao [1] discovered that GPS disposal orbits can be unstable and undergo significant eccentricity growth over a time frame of decades. The cause of this long-term eccentricity growth is a dynamical resonance condition resulting from the combined gravitational pull of the sun, moon, and the nonspherical gravity field of the Earth (primarily the J_2 zonal harmonic). Gick and Chao [2] showed that the amount of eccentricity growth depends on the initial elements of the disposal orbit. Chao and Gick [3] also showed that disposal orbits for other systems in MEO (i.e., GLONASS and Galileo) can be unstable. Jenkin and Gick [4,5] performed analyses of the long-term collision risk posed to the operational GPS constellation by vehicles disposed 500 and 832 km above the ideal GPS semisynchronous orbit. These orbits can repenetrate the constellation due to long-term eccentricity growth.

The purpose of the study presented here is to determine the long-term collision risk posed to the GPS constellation by disposed EELV upper stages that are not fully removed from the constellation. The long-term eccentricity growth of the disposal orbits has an important effect on long-term collision risk, and it is therefore considered in the analysis. Only one version of the launch vehicle was considered here.

II. Disposal Orbit Initial Conditions

The upper-stage disposal orbit initial conditions determine the long-term eccentricity growth and hence the long-term collision risk. Gick and Chao [2] showed that long-term eccentricity growth of a disposal orbit is primarily determined by the initial orbit eccentricity, argument of perigee, and right ascension of ascending node (RAAN). The eccentricity and argument of perigee are determined by the launch vehicle and upper-stage performance. The RAAN is determined by the orbit plane in which the upper stage is deposited.

After the upper stage has injected the GPS satellite into a drift orbit within the constellation, it will separate from the satellite and then perform several operations that impart a ΔV, thereby modifying the orbit of the upper stage. These operations include a contamination and collision avoidance maneuver (CCAM), propellant blowdown, and hydrazine depletion burn. The amount of ΔV that is imparted is determined by the residual propellant and hydrazine available, and these residuals in turn vary with launch vehicle performance dispersions.

Only one version of the EELV upper stage was considered in the study presented here. For this version, the variation in the imparted ΔV by the combined CCAM/blowdown/depletion procedure can be large enough to cause significant variation in initial eccentricity of the final disposal orbit, thereby affecting eccentricity growth. It can also cause significant variation in the locations of perigee and apogee relative to the constellation altitude band, and therefore directly impact collision risk. As a result, it is necessary to model the variation in the imparted ΔV.

A Monte Carlo procedure was developed to model the effect of the variation in the combined CCAM/blowdown/depletion ΔV on the initial disposal orbit. The basis for this model was performance simulation data that were supplied by the builder of the launch vehicle. These data showed final disposal orbit elements for various stacked combinations of separate ΔV dispersion sources at nominal, three-sigma high and three-sigma low levels. The Monte Carlo model consisted of a random total ΔV that is a linear combination of multiple random ΔV sources. Each ΔV source had either a uniform or Gaussian distribution. The parameters of the probability distributions of the individual ΔV source components were selected from nominal, three-sigma high, three-sigma low, and max range ΔV values for each source supplied by the builder. For each Monte Carlo instance, the change imparted to disposal orbit apogee and perigee altitude by the combined CCAM/blowdown/depletion ΔV was then determined by multiplying the nominal change in apogee and perigee altitude by the ratio of the random instance of total ΔV to nominal total ΔV. This procedure effectively prorates the change in apogee and perigee altitudes by the deviation in ΔV from its nominal value. This linear proration procedure is simple yet accurate because the changes to apogee and perigee altitude due to the ΔV perturbation are well within the range of linear variation. The number of Monte Carlo initial conditions was varied to assess the sensitivity of the profiles of total collision probability that are generated at the end of the analysis. After trying up to 10,000 Monte Carlo trials, it was found that the total collision probability profiles converged for 1000 Monte Carlo instances. Because the long-term propagation of the disposal orbit initial conditions becomes computationally expensive for more than 1000 iterations, the final cases were run with 1000 Monte Carlo instances of disposal orbit initial conditions.

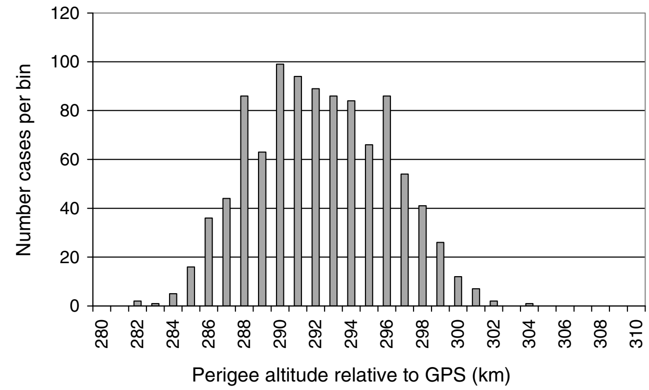

Fig. 1 Histogram of perigee altitudes of initial upper-stage disposal orbits (bin width = 1 km).

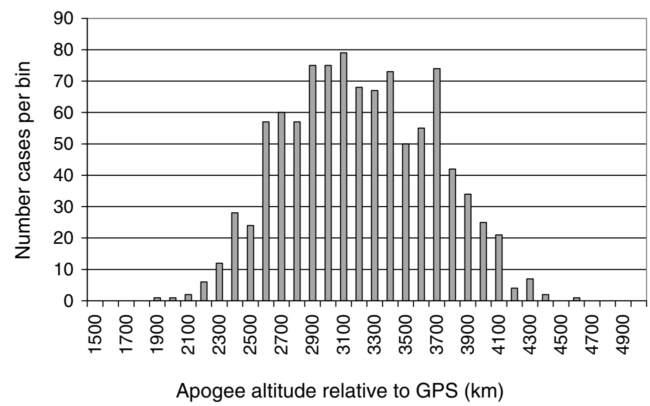

Fig. 2 Histogram of apogee altitudes of initial upper-stage disposal orbits (bin width = 1 km).

The resulting distributions of perigee and apogee relative to the ideal GPS semisynchronous orbit are shown in the form of histograms in Figs. 1 and 2. The perigee varies at most by only 20 km. However, the apogee can vary from 1800 to 4500 km. This wide range in the apogee significantly affects the relative amount of time spent by the upper stage in the constellation, and therefore it directly affects collision risk.

Even at its lowest value, the apogee altitude is much higher than the perigee altitude (relative to the ideal GPS semisynchronous orbit). As a result, the argument of perigee is mostly determined by the argument of latitude of the upper stage at the centroid of the combined CCAM/blowdown/depletion maneuver. In this study, an injection at the ascending node of the constellation orbit plane was assumed, and the argument of perigee was therefore assumed to remain fixed at zero. The performance simulation data showed that the actual argument of perigee deviates from zero at most by 20 deg.

The upper-stage disposal orbit RAANs were randomly selected from the RAANs of the six constellation planes at epoch 1 August 2001. The actual values of RAAN will depend upon the disposal epoch due to the effect of nodal regression induced by the J_2 zonal harmonic of the Earth's gravity field. At an expected average disposal rate of 2.33 upper stages per year, 12 missions will span 4.7 years. At a nodal regression rate of 0.04 deg/day, the orbit planes will regress 69 deg, which is more than the RAAN spacing of 60 deg between subsequent planes. Therefore, 12 disposed upper stages could potentially have RAANs that span the full 360 deg range. The selection of six discrete RAAN values for the analysis therefore represents a coarse sampling of the full 360 deg possible range. This coarse sampling procedure was selected to expedite the analysis. Subsequent analysis using finer sampling of the 360 deg RAAN range has shown that the usage of six discrete RAAN values yields an effective representation of the entire range of eccentricity growth profiles as determined by the disposal orbit RAAN.

The initial inclination of the upper-stage disposal orbits was assumed to be the nominal constellation value of 55 deg. The initial mean anomaly was assumed to be zero. Neither of these quantities, within their dispersion ranges, has a strong effect on eccentricity growth. The mean anomaly, in particular, is of little significance because the long-term evolution of mean anomaly is highly sensitive to dispersions in the semimajor axis. The semimajor axis in turn varies significantly due to the large apogee altitude variation. Therefore, mean anomaly (and hence argument of latitude) cannot be predicted with any accuracy over decades and is essentially random over 360 deg. The collision risk analysis discussed next accounts for this randomness in mean anomaly.

III. Disposal Orbit Evolution

The upper-stage disposal orbit long-term mean element histories over 200 years were computed using the long-term orbit control tool MEANPROP. The executive driver of MEANPROP, which includes modeling orbit control, was developed in-house. To model natural orbital evolution, MEANPROP calls the Semi-Analytic Orbit Propagator (SAOP), a program developed by the Charles Stark Draper Laboratory that has undergone extensive validation [6]. All pertinent perturbations were modeled: sun-moon gravity, solar radiation pressure, and an 8×8 WGS84 Earth gravity field.

As a sample of the overall results, Fig. 3 shows the corresponding time profiles of perigee and apogee altitude, relative to the GPS constellation altitude band, for six randomly selected initial disposal orbits. In the figure, the lower six curves show the perigee altitude histories for the six cases. The higher six curves show the apogee altitude histories. The relative presence of the upper stage in the constellation altitude band is dependent on the perigee and apogee altitudes of its orbit. As can be seen from Fig. 3, the presence of the upper stage in the constellation altitude band varies considerably across the six cases. The actual collision risk for these cases is presented in the next section.

IV. Constellation Model

The constellation model used in this study is the same as that used in the study of Jenkin and Gick [5]. The way it was generated is presented again here due to its importance for the current study.

To account for the orbital configuration of the constellation over the 200-year time period addressed by this study, the mean elements of 28 constellation slots were propagated using MEANPROP. The initial conditions of the vehicle slots were generated from mean element data that were derived from osculating Mission Control Segment (MCS) state vectors dated 14 August 2000 and propagated to an epoch of 1 August 2001.

GPS station keeping maneuvers were not modeled because they have little influence on eccentricity compared to orbital perturbations. Therefore, the longitude of ascending node was allowed to drift in the propagation runs. In this case, the effect of tesseral gravity harmonics on the long-term evolution of eccentricity is different than when the longitude of ascending node is held constant by stationkeeping. However, it was shown during the study that the impact on the overall statistical spread of eccentricity over 100 years is very small when stationkeeping is disabled, and therefore it was neglected for this study.

It is also not necessary to model stationkeeping because the in-track position has no effect on long-term collision probability. The formulation of collision probability used in this study (described later) is based on the assumption that the in-track position (i.e., argument of latitude) of the disposed upper stage relative to the satellite is continually randomized over 360 deg. This assumption is valid due to the significant difference between the semimajor axes of the disposed upper stage and satellite, which is caused by the high upper-stage disposal orbit apogees. This difference in semimajor axes causes a large enough difference in orbital mean motions to produce continual recirculation of the upper stage relative to the satellite over 360 deg with a repeat period of days to weeks (depending on the disposal orbit semimajor axis).

To model the discontinuity in eccentricity of each slot due to the replacement of vehicles at end of life, the eccentricity was periodically rectified back to an initial value of 0.008 every 15 years. A replacement period of 15 years was selected to allow for maximum eccentricity growth, and hence altitude spread of the constellation.

Over a 200-year time span, a statistical model of the spatial distribution of the constellation satellites was generated to support the collision risk analysis in this study. More specifically, the spatial number density as a function of altitude, averaged over 200 years, was computed. This spatial density distribution was determined as follows. The spatial density distribution over altitude for each constellation slot at each time in the MEANPROP long-term propagation files was computed using the formulation of satellite altitude distribution derived by Dennis [7]. This formulation is equivalent to the one derived by Kessler [8]. The satellite latitude distribution was not included in the computation of the spatial density distribution for each constellation slot at each time point. These spatial density distributions were then averaged across all the constellation slots and propagation time points over 200 years. Figure 4 shows the resulting average spatial density distribution over altitude $\rho(h)$. It can be seen from this figure that the disposal regions recommended by the U.S. Government Debris Mitigation Standard Practice clear the majority of the altitude band occupied by the GPS Block IIF constellation.

V. Collision Risk Analysis

In previous work by the authors [4], collision risk posed to the GPS constellation by disposed vehicles was computed using a direct statistical analysis of miss distances generated by simulation of conjunctions over 200 years. This was justified by showing that, for the cases simulated, the differences between the mean motions of the

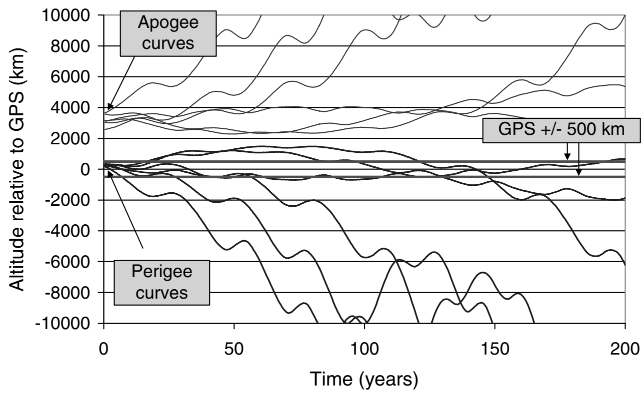

Fig. 3 Perigee and apogee altitude vs time profiles for six randomly selected initial upper-stage disposal orbits.

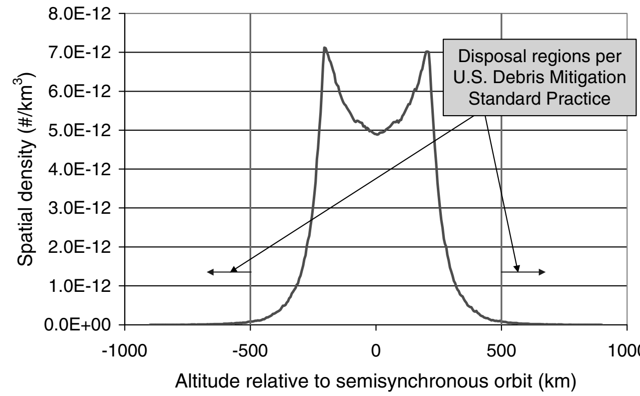

Fig. 4 Variation of spatial number density of the GPS constellation over altitude, averaged over latitude and 200 years.

orbits of the satellites and disposed vehicles allow for complete randomization of the miss distances at subsequent conjunctions over a period of a couple years. Therefore, a single conjunction simulation over 200 years was guaranteed to produce a statistically significant set of miss distances from which a miss distance probability distribution could be determined. This procedure enabled an accurate determination of collision risk.

The drawback of the miss distance-based method is that the conjunction simulation of 200 years is computationally intensive. Whereas it was successfully applied to the small number of disposal orbits considered in [4] (essentially six different values of RAAN for the six constellation planes), it was not feasible to apply this method to the current study, which involves 1000 Monte Carlo variates of the upper-stage disposal orbit initial conditions.

For the current study, a density-based method was used to compute collision risk. This method is formulated from the perspective of the disposed upper stage as it flies through the constellation spatial density field. The generalized formulation is

$$N_C(t) = A_{\mathrm{cc}} \int_{t_0}^{t} \rho[r_{\mathrm{us}}(\tau)] v \, \mathrm{d}\tau \tag{1}$$

$$p_C(t) = 1 - e^{-N_C(t)} \tag{2}$$

In this study, the value of A_{cc} was computed from the collision radius R_{cc} as $A_{\mathrm{cc}} = \pi R_{\mathrm{cc}}^2 = 149\ \mathrm{m}^2$. The corresponding collision radius $R_{\mathrm{cc}} = 6.89$ m was an estimate of the average of collision radii that permit any physical contact between the Block IIF satellite and EELV upper stage, thereby causing potential damage to the satellite.

To accelerate the computer processing of the 1000 Monte Carlo disposal cases, the integration in Eq. (1) was implemented using the method of averaging. This involves separating the problem into a short time-scale problem and a long time-scale problem. The short time-scale problem consists of determining the average number of collisions over a single orbit revolution. The long time-scale problem consists of using the collision risk evaluated for a sampling of orbital revolutions to compute the cumulative collision risk for all revolutions. The computational savings is realized by avoiding the computation of the collision risk for each individual orbital revolution.

The average number of collisions over a single orbit revolution is computed for a single instance of mean orbital elements that are propagated to a given epoch t_L by MEANPROP by carrying out the integration of Eq. (1) over the short time scale of one orbital period. The resulting average number of collisions per revolution is then divided by the orbit period to yield the average rate of growth of average number of collisions at the given mean orbital element epoch t_L.

$$\left\langle \frac{\mathrm{d}N_C}{\mathrm{d}t} \right\rangle (t_L) = \frac{1}{T_p} A_{\mathrm{cc}} \int_0^{T_p} \rho\{h_{\mathrm{us}}[\tau_S, x(t_L)]\} v \, \mathrm{d}\tau_S \tag{3}$$

where $h_{\mathrm{us}}[\tau_s, x(t_L)]$ is the altitude of the upper stage at short time-scale point τ_s during a given orbital revolution ($\tau_s = 0$ corresponds to perigee) for mean orbital elements in the vector x at the long time-scale point t_L. The variation of h_{us} with τ_s at fixed t_L is modeled via Keplerian motion. A value of 4.86 km/s was used for the average relative velocity v. This value was determined by computing the difference in velocity vectors at the nodal crossings between all pairs of constellation orbits and averaging the resulting values.

The cumulative number of collisions up to the mean orbital element epoch t_L is then determined by integrating Eq. (3) over the long time scale.

$$N_C(t_L) = \int_{t_0}^{t_L} \left\langle \frac{\mathrm{d}N_C}{\mathrm{d}\tau} \right\rangle (\tau_L) \, \mathrm{d}\tau_L \tag{4}$$

A computer program was developed that evaluates Eq. (3) at each time point t_L in the mean orbit element histories. It then evaluates the integral in Eq. (4) [and subsequently Eq. (2)] via a discrete trapezoidal algorithm that processes the results of Eq. (3) at those time points. This program was used to generate profiles of cumulative collision probability vs time for each instance of the statistical ensemble of initial upper-stage disposal orbit conditions.

The drawback of the density-based method is that it is less accurate than the miss distance-based method. It does not account for the correlations that exist between the upper-stage disposal orbit and the constellation satellite orbits. In particular, there are correlations between the two orbit classes in the RAANs and arguments of perigee because they evolve slowly, especially relative to each other. However, the RAANs of the constellation planes are uniformly spaced as a whole (albeit deterministically and not randomly), and the initial values of arguments of perigee of the constellation slots are randomly distributed throughout the constellation. As a result, the accuracy loss of the density-based method is not severe.

To demonstrate this fact, a numerical comparison between the two methods was performed for a case taken from [5]. In this case, six vehicles are disposed in orbits with perigee 500 km above the ideal GPS semisynchronous altitude and initial eccentricity of 0.005, with one vehicle in each constellation plane. These vehicles subsequently penetrate the constellation due to orbital eccentricity growth. Using each method, the collision probability time profiles over 200 years were computed and then averaged together into a single profile. The averaged profiles resulting from the two methods are presented in Fig. 5. This plot shows that, for the case considered, the density-based method generated a collision probability profile that is higher than that computed by the miss distance-based method by a factor of at most 1.4. Given other uncertainties in the problem (constellation configuration, satellite replacement rates, disposal orbit initial conditions, collision radii), this deviation is considered to be acceptable for this study.

Figure 6 shows the resulting collision risk profiles corresponding to the six upper-stage disposal orbit perigee and apogee altitude profiles presented in Fig. 3. Figure 7 shows the apogee and perigee time history for the case with lowest collision risk over the time interval from 120 to 160 years. In this case, the perigee actually rises

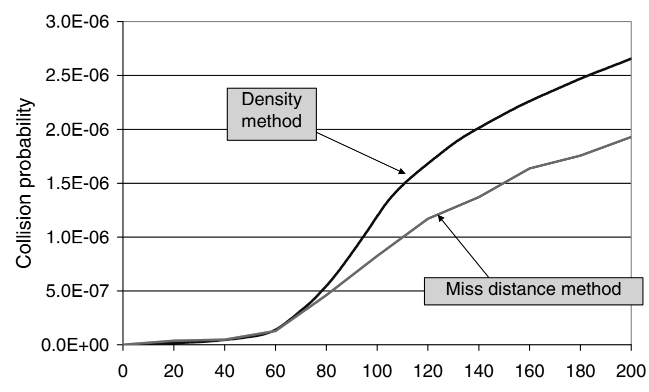

Fig. 5 Comparison of methods for computing collision risk.

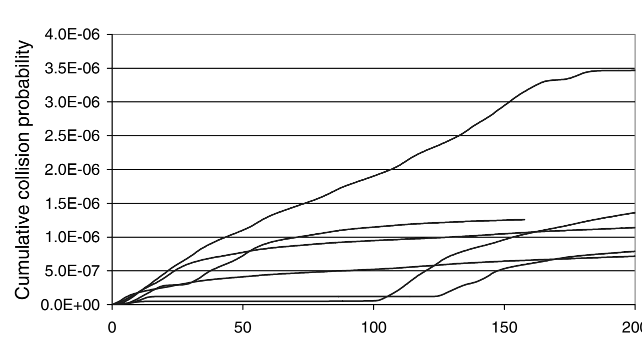

Fig. 6 Collision probability vs time profiles corresponding to the six perigee and apogee altitude vs time profiles presented in Fig. 3.

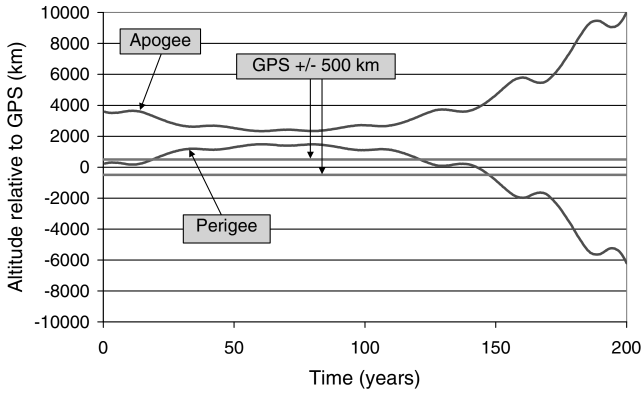

Fig. 7 Perigee and apogee altitude vs time profiles for the case with lowest collision risk among the six sampled Monte Carlo cases over the time interval from 120 to 160 years.

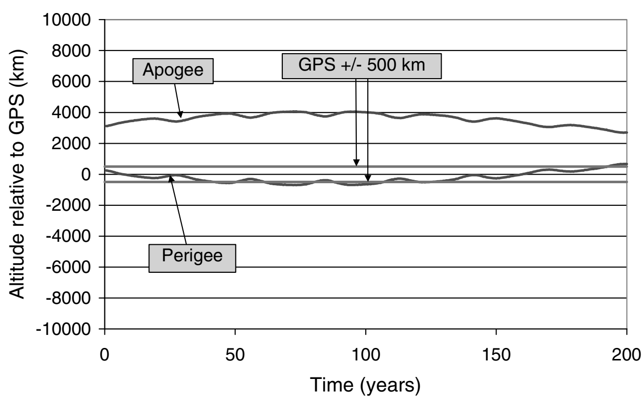

Fig. 8 Perigee and apogee altitude vs time profiles for the case with highest collision risk among the six sampled Monte Carlo cases.

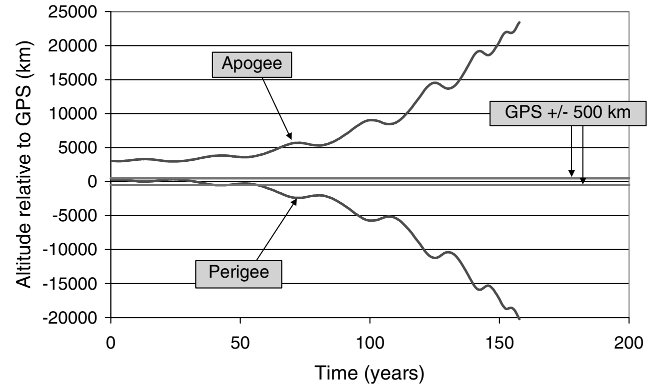

Fig. 9 Perigee and apogee altitude vs time profiles for the case with highest eccentricity growth among the six sampled Monte Carlo cases.

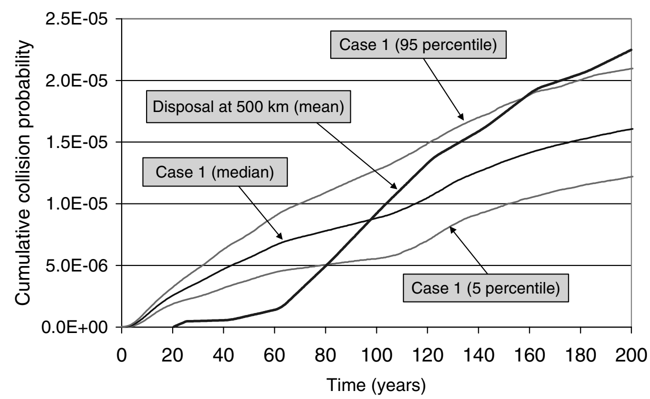

Fig. 10 Cumulative collision risk over time posed to the constellation by 12 disposed upper stages (Case 1).

and remains above the constellation altitude band for 120 years. Subsequently, the perigee dips back and passes through the constellation altitude band. The corresponding collision probability remains low for the first 120 years, and then grows rapidly. Figure 8 shows the apogee and perigee time history for the case with highest collision risk at the end of the 200-year period. In this case, the perigee remains within the constellation altitude band for most of the 200-year period. The corresponding collision probability grows steadily throughout most of the 200-year period. Figure 9 shows the apogee and perigee time history corresponding to the collision risk curve in Fig. 6 that stops at approximately 160 years. This is also the case with highest eccentricity growth by the end of the 200-year period. In this case, the perigee dips below the constellation altitude band roughly within the first 50 years and continues to accelerate downward until reentry occurs at approximately 160 years. While the upper stage remains present in the constellation altitude band, the spreading perigees and apogees reduce the time spent by the upper stage in the constellation altitude band, thereby diluting the growth rate of collision risk. This is demonstrated by the fact that the corresponding collision risk is less than the collision risk corresponding to the case in which the perigee remains within the constellation altitude band for most of the 200-year period.

VI. Simulation of the Disposal Process

The disposal of individual upper stages will be spread out over time as replacement satellites are injected into the constellation. In this study, the upper-stage disposal process was modeled via a fixed disposal rate of 2.33 per year. Two cases were considered. In Case 1, a total of 12 upper stages will be left with perigees residing in the constellation altitude band. After that, all future upper stages will be completely removed from the constellation altitude band. Case 2 consists of a hypothetical scenario in which all future upper stages over the next 200 years are left with perigees residing in the constellation altitude band.

The simulation steps through each disposal event one by one through time. At each time point, an instance from the statistical ensemble of upper-stage disposal orbit initial conditions is randomly selected and the corresponding collision risk time profile is extracted. The entire profile is shifted in time (delayed) so that it starts at the current disposal time point. The shifted collision risk time profile is then added to a running cumulative time profile of total collision risk that continues out to a time point 200 years after the first disposal event.

The entire sequence of disposal events from beginning to end is then itself repeated 1000 times in Monte Carlo fashion. This permits a statistical quantification of the potential variability in the total collision risk vs time. For each disposal sequence, the resulting total collision risk at each time point through 200 years is placed in a histogram bin. After the 1000 Monte Carlo disposal sequences are completed, the median value and the 5- and 95-percentile values are computed from the histogram at each time point.

The resulting time profiles are shown in Fig. 10 for Case 1. For a total of 12 disposed upper stages, it is seen that the there is a wide spread between the 5- and 95-percentile profiles. Therefore there is significant variability in the total collision risk due to the uncertainties in the disposal process. However, the absolute collision risk is low. Even after 200 years, the total collision risk posed by all 12 upper stages to the constellation will be less than 2.1×10^{-5} (1 in 47,000) with 95% confidence. Therefore the deposition of upper stages in the constellation does not pose a significant collision risk to the constellation as long as the number of stages left is restricted to 12.

The results for Case 2 are shown in Fig. 11. It is seen that there is a much narrower spread between the 5- and 95-percentile profiles than for Case 1. This is due to the much greater number of disposed upper stages: the effects of the random variations in the disposal orbit initial

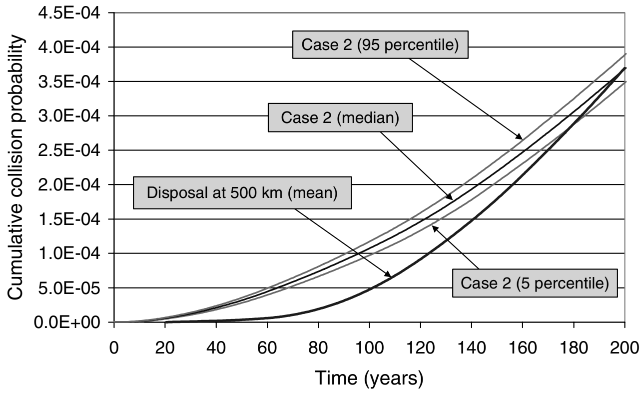

Fig. 11 Cumulative collision risk over time posed to the constellation by all disposed upper stages over 200 years (Case 2).

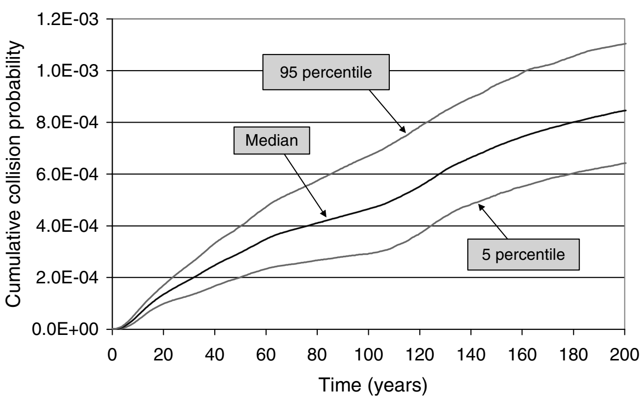

Fig. 12 Cumulative collision risk over time posed to the constellation by 12 disposed upper stages (Case 1): collision radius = 50 m.

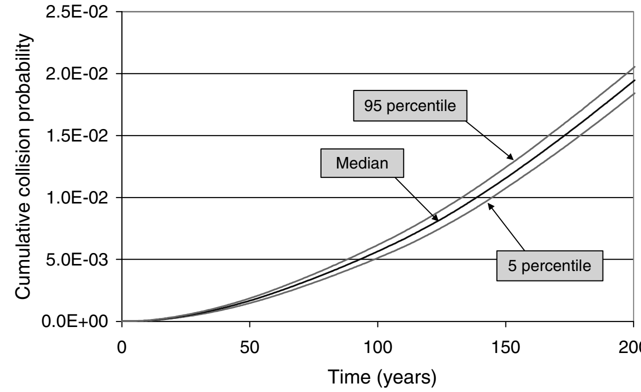

Fig. 13 Cumulative collision risk over time posed to the constellation by all disposed upper stages over 200 years (Case 2): collision radius = 50 m.

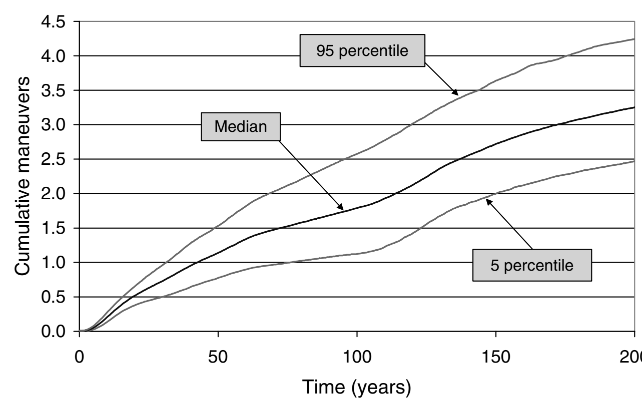

Fig. 14 Cumulative maneuvers over time imposed on the constellation by 12 disposed upper stages (Case 1).

conditions tend to average out as the number of disposal events increases. It is also seen that the absolute collision risk is still low. After 200 years, the median risk is 3.6×10^{-4}, and is no greater than 4.0×10^{-4} (1 in 2500) with 95% confidence.

In [4], the authors determined the collision risk posed to the constellation after 180 years by satellites and upper stages placed in disposal orbits with a perigee at 500 km and an initial eccentricity of 0.005. That study assumed that the only eccentricity control strategy used is minimization of initial eccentricity, and not targeting of the argument of perigee [2]. Figures 10 and 11 each contain a curve that shows the collision risk from that study recomputed for the upper-stage populations and the updated collision radius used in the current study. It is seen that, for both cases, the total collision risk over 200 years for the upper-stage disposal orbits considered in this study is initially greater than the collision risk that would be posed by the upper stages had they been moved to the 500-km-disposal orbits. However, eventually the collision risk posed by the upper stages had they been moved to the 500-km-disposal orbit would become greater.

The reason for this result is that the perigees of the upper stages considered in this study are initially below 500 km and reside within the constellation altitude band, thereby resulting in greater immediate collision risk than if they had been disposed in the 500-km-disposal orbits. However, due to their high initial eccentricities, the disposal orbits of the upper stages considered in this study have more rapid eccentricity growth than the 500-km-disposal orbits. Disposed upper stages with higher orbital eccentricity spend a smaller fraction of time in the constellation altitude band than disposed upper stages with lower orbital eccentricity, thereby diluting the rate of accumulation of collision risk.

The collision risk results of the study are contingent upon the underlying assumptions, including constellation configuration and collision radii. In particular, as the constellation design evolves, the size of the spacecraft may change significantly. One possibility is that the satellites may increase in size as they are designed with increasing capabilities. To consider this effect, the collision risk profiles were regenerated assuming a collision radius of 50 m. Figures 12 and 13 show the resulting collision risk time profiles for Cases 1 and 2, respectively. It is seen that the collision risk has increased significantly. For Case 1, the absolute risk is still relatively low. The collision risk remains below 1 in 1000 for roughly 160 years with 95% confidence. For Case 2, the same threshold has been exceeded after 50 years. After 100 years, the collision risk will be *at least* 1 in 200 with 95% confidence.

In addition to collision risk, the collision avoidance maneuver frequency is also of interest, because avoidance maneuvers may induce outages in satellite operation. In addition to being related to the collision risk, maneuver frequency is also a function of orbit determination accuracy for the disposed upper stage. As the position error ellipsoid about an upper stage increases in size, avoidance maneuvers must occur at larger miss distances to achieve clearance at a given level of confidence. In this study, it is assumed that tracking technology will be sufficiently accurate over the next 200 years so that maneuvers will be triggered when predicted miss distance at conjunction is 3.1 km or less. It is noted that this is a rough estimate. Any actual future maneuver threshold miss distance will be determined by a combination of tracking technology accuracy and operator sensitivity to risk.

The maneuver frequency time profiles can then be computed by multiplying the collision risk time profiles by the ratio $(R_m/R_{cc})^2$, where $R_m = 3.1$ km is the maneuver radius. This simple proration caries directly over to the median, 5-, and 95-percentile time profiles. The results are shown in Figs. 14 and 15. For Case 1, the first maneuver will not be induced for at least 28 years with 95% confidence, and no more than three maneuvers are expected after 115 years with 95% confidence. For Case 2, no more than 25 maneuvers are expected after 100 years with 95% confidence.

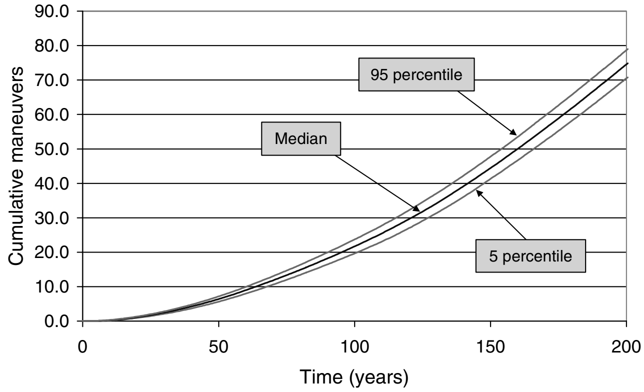

Fig. 15 Cumulative maneuvers over time imposed on the constellation by all disposed upper stages over 200 years (Case 2).

It is noted that this study is limited to considering the collision risk posed directly to the relatively small number of 28 satellites in the constellation. There are many more objects in the MEO region, including the GLONASS system and objects transiting on highly eccentric orbits. There would also be many disposed upper stages that pose a collision risk to each other. The risk of collision among these objects, and the resulting risk posed to the constellation by the millions of debris fragments that would be produced by such collisions, has not yet been addressed.

VII. Summary and Conclusions

A study was performed to determine the long-term collision risk posed to the GPS constellation by upper stages that will be left in the constellation by the EELVs that launch Block IIF satellites. The study accounted for the sensitivity of upper-stage disposal orbit long-term eccentricity growth to the uncertainty in initial disposal orbit conditions. This uncertainty is caused by launch vehicle and upper-stage performance dispersions, as well as by the inability to predict in advance the sequence of constellation planes in which the upper-stage disposal will occur. A Monte Carlo procedure was used to model the effect of disposal orbit uncertainty on long-term collision risk. Only one version of the launch vehicle was considered here.

Two cases were considered. In Case 1, a maximum of 12 upper stages are left in the constellation. In Case 2, all future upper stages are left in the constellation. For Case 1, the study showed that the collision risk remains below 2.1×10^{-5} (1 in 47,000) over 200 years with 95% confidence. For Case 2, the study showed that the collision risk remains below 4.0×10^{-4} (1 in 2500) over 200 years with 95% confidence. These collision risk values are based on the collision radius of 6.89 m that was estimated to permit physical contact between a Block IIF satellite and an EELV upper stage. Results were also generated for a case in which the size of the satellites increases in the future. For a collision radius of 50 m, the collision risk remains low for Case 1. However, in Case 2, collision risk exceeds 1 in 1000 after 50 years, and after 100 years the collision risk is *at least* 1 in 200 with 95% confidence. The expected number of collision avoidance maneuvers appears to be manageable for both cases when assuming a maneuver radius of 3.1 km.

The study showed that the total collision risk over 200 years for the upper-stage disposal orbits considered in this study is initially greater than the collision risk that would be posed by the upper stages had they been moved to disposal orbits with a perigee at 500 km above the ideal GPS semisynchronous orbit and with an initial eccentricity of 0.005 to reduce eccentricity growth. However, eventually the collision risk posed by the upper stages had they been moved to the 500-km-disposal orbit would become greater. The reason for this result is that the disposal orbits of the upper stages considered in this study have high initial eccentricities, which result in more rapid eccentricity growth than the 500-km-disposal orbits. The faster eccentricity growth eventually causes dilution of the rate of accumulation of collision risk. Therefore, the high initial eccentricities of the upper-stage disposal orbits eventually help to offset the immediate increase in collision risk caused by leaving the initial perigees in the constellation altitude band.

The study did not consider the risk of collision among the upper stages themselves, or with background objects, and the associated risk posed to the constellation by the millions of debris fragments that would be produced by such collisions. It is planned to address this risk in subsequent work.

Acknowledgments

This work reflects research conducted under U.S. Air Force and Missile Center Contract F04701-93-C-0094. The authors wish to thank several individuals at The Aerospace Corporation for their support of this work and assistance in preparing this paper. J. E. Gidney provided GPS-specific technical and programmatic consultation. H. J. Schraibman and J. R. Berg of the GPS Program Office provided internal support for this work. D. Q. Truong provided programmatic assistance from the EELV Program Office. J. E. Gidney, C. C. Chao, H. J. Schraibman, and D. Q. Truong provided thorough technical and programmatic review of the paper. The following individuals provided programmatic support for paper presentation at the conference: J. M. Wyrwitzke, H. N. Nguyen, N. Chen, W. H. Ailor, D. Q. Truong, L. B. Crosse, and J. R. Berg.

References

[1] Chao, C. C., "MEO Disposal Orbit Stability and Direct Reentry Strategy," *Advances in the Astronautical Sciences*, Vol. 105, Jan. 2000, pp. 817–838.

[2] Gick, R. A., and Chao, C. C., "GPS Disposal Orbit Stability and Sensitivity Study," *Advances in the Astronautical Sciences*, Vol. 108, Feb. 2001, pp. 2005–2018.

[3] Chao, C. C., and Gick, R. A., "Long-Term Evolution of Navigation Satellite Orbits: GPS/GLONASS/GALILEO," *Advances in Space Research*, Vol. 34, No. 5, 2004, pp. 1221–1226.

[4] Jenkin, A. B., and Gick, R. A., "Collision Risk Posed to the Global Positioning System by Disposal Orbit Instability," *Journal of Spacecraft and Rockets*, Vol. 39, No. 4, July–Aug. 2002.

[5] Jenkin, A. B., and Gick, R. A., "Collision Risk Associated with Instability of MEO Disposal Orbits," *Proceedings of the Third European Conference on Space Debris*, SP-473, edited by H. Sawaya-Lacoste, Vol. 1, ESA, Darmstadt, Germany, Oct. 2001, pp. 471–476.

[6] McClain, W. D., "A Recursively Formulated First-Order Semianalytic Artificial Satellite Theory Based on the Generalized Method of Averaging," Computer Sciences Corporation, CSC/TR-77/6010, Greenbelt, MD, Nov. 1977.

[7] Dennis, N. G., "Probabilistic Theory and Statistical Distribution of Earth Satellites," *Journal of the British Interplanetary Society*, Vol. 25, 1972, pp. 333–376.

[8] Kessler, D. J., "Derivation of the Collision Probability Between Orbiting Objects: The Lifetimes of Jupiter's Outer Moons," *Icarus* Vol. 48, 1981, pp. 39–48.

J. Korte
Associate Editor